An Approach to Determining an Equivalent Circuit for HEMT's

Kazuo Shirakawa, Hideyuki Oikawa, Toshihiro Shimura, Yoshihiro Kawasaki, Yoji Ohashi, Tamio Saito, *Member, IEEE,* and Yoshimasa Daido, *Member, IEEE*

***Abstract*—A simple way to determine a small-signal equivalent circuit of High Electron Mobility Transistors (HEMT's) is proposed. Intrinsic elements determined by a conventional analytical parameter transformation technique are described as functions of extrinsic elements. Assuming that the equivalent circuit composed of lumped elements is valid over the whole frequency range of the measurements, the extrinsic elements are iteratively determined using the variance of the intrinsic elements as an optimization criterion. Measurements of S-parameters up to 62.5 GHz at more than 100 different bias points confirmed that the HEMT equivalent circuit is consistent for all bias points.**

I. Introduction

DESIGNING nonlinear components such as high power amplifiers requires accurate nonlinear characteristics of active devices [1], [2].

Empirical methods like load-pull [3], [4] can be used at relatively low frequencies, but the equivalent circuit approach is better suited at millimeter wave frequencies because it is free from experimental problems. Conventionally, values of equivalent circuit elements are determined using optimizers which come with commercially available software. These optimizers do not, however, check whether a circuit is valid, and are not therefore consistent over all operating bias points. The choice of the initial values for optimization also affects the results [2], [5], [6].

Improvements have been proposed for GaAs MESFET's, but they commonly need extra measurements at DC, very low frequencies, and in a cold state to determine extrinsic elements [6]–[9].

In this paper, we describe a technique to determine a HEMT equivalent circuit which requires no additional measurements. Our technique is the first step towards developing a nonlinear model for HEMT's. Intrinsic elements determined by a conventional analytical parameter transformation technique are expressed as functions of extrinsic elements. Assuming that the equivalent circuit composed of lumped elements is valid over the whole frequency range of the measurements, the extrinsic elements are iteratively determined using the variance of the intrinsic elements as an optimization criterion. The extrinsic elements are strongly constrained by the variance, and the choice of the initial values for optimization little affects the results.

Manuscript received November 10, 1993; revised May 27, 1994.

K. Shirakawa, T. Shimura, Y. Kawasaki, Y. Ohashi, T. Saito, and Y. Daido are with Fujitsu Laboratories Ltd., Kawasaki 211, Japan.

H. Oikawa is with Fujitsu Tohoku Digital Technology Ltd., Sendai 980, Japan.

IEEE Log Number 9407459.

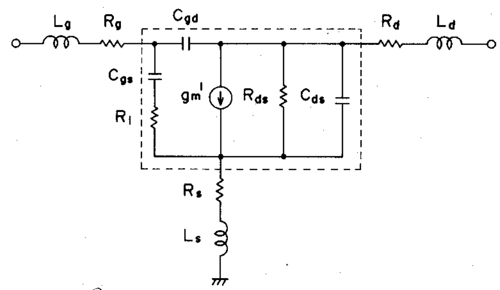

Fig. 1. Equivalent circuit of GaAs MESFET. Inside the dashed-line denotes the intrinsic part, and outside is the extrinisic part: $g'_m = g_m \exp(-j\omega t)$.

We measured S-parameters of a HEMT up to 62.5 GHz, at more than 100 different bias settings, and determined the intrinsic elements at each bias point. We checked the consistency of the resulting HEMT equivalent circuit for all bias points using the frequency characteristics of the intrinsic elements.

II. Equivalent Circuit

Many equivalent circuits have been proposed for HEMT's, but the simple conventional equivalent circuit for MESFET's (Fig. 1) is still one of the most useful.

The intrinsic part of the device (surrounded by the dashed-line in Fig. 1) is described by a Y matrix as:

$$Y_{int} = \begin{bmatrix} Y_{11} & Y_{12} \\ Y_{21} & Y_{22} \end{bmatrix} = \begin{bmatrix} \dfrac{j\omega C_{gs}}{1+j\omega C_{gs}R_i} + j\omega C_{gd} & -j\omega C_{gd} \\ \dfrac{g_m e^{-j\omega\tau}}{1+j\omega C_{gs}R_i} - j\omega C_{gd} & g_{ds} + j\omega(C_{gd}+C_{ds}) \end{bmatrix}. \quad (1)$$

At millimeter wave frequencies, measured data tend to suffer from unpredictable parasitic elements. RF wafer probe measurements using TRL (Thru-Reflection-Line) calibration reduces the extrinsic elements as shown in Fig. 1.

The extrinsic part is then described by a Z matrix (2), shown at the bottom of the next page.

Complete device Z-parameters, Z_t, are the sum of Z_{ext} and the reciprocal of Y_{int},

$$Z_t = Z_{ext} + Y_{int}^{-1}. \tag{3}$$

III. Analytical Determination of Equivalent Circuit

A. Intrinsic Elements

With the equivalent circuit in Fig. 1, we can determine its intrinsic elements analytically. From (3), the measured S-parameters are converted to Z-parameters and the extrinsic elements subtracted. Then the remaining Z-parameters are converted to Y-parameters, and using (1), the intrinsic elements are determined at each frequency point as follows:

$$d(\omega_i) = \frac{\mathrm{Re}\,(Y_{11}(\omega_i) + Y_{12}(\omega_i))}{\mathrm{Im}\,(Y_{11}(\omega_i) + Y_{12}(\omega_i))} \tag{4}$$

$$c(\omega_i) = (Y_{21}(\omega_i) - Y_{12}(\omega_i))(1 + j\omega_i\, d(\omega_i)) \tag{5}$$

$$C_{gs}(\omega_i) = \frac{(1 + d^2(\omega_i))}{(\omega_i)}\,\mathrm{Im}\,(Y_{11}(\omega_i) + Y_{12}(\omega_i)) \tag{6}$$

$$R_i(\omega_i) = \frac{d^2(\omega_i)}{(1 + d^2(\omega_i)\,\mathrm{Re}\,(Y_{11}(\omega_i) + Y_{12}(\omega_i))} \tag{7}$$

$$C_{gd}(\omega_i) = \frac{-\mathrm{Im}\,(Y_{12}(\omega_i))}{\omega_i} \tag{8}$$

$$g_m(\omega_i) = \sqrt{c^2(\omega_i)} \tag{9}$$

$$\tau(\omega_i) = -\frac{1}{\omega_i}\tan^{-1}(\mathrm{Im}\,(c(\omega_i)), \quad \mathrm{Re}\,(c(\omega_i))) \tag{10}$$

$$g_{ds}(\omega_i) = \mathrm{Re}\,(Y_{22}(\omega_i) + Y_{12}(\omega_i)) \tag{11}$$

$$C_{ds}(\omega_i) = \frac{\mathrm{Im}\,(Y_{22}(\omega_i) + Y_{12}(\omega_i))}{\omega_i} \tag{12}$$

where ω is the angular frequency and i (= 0, $\cdots$, $N-$ 1) is the number of sampling points.

B. Effect of Extrinsic Elements on Determining Intrinsic Elements

As the previous section described, once extrinsic elements are obtained, intrinsic elements can be determined analytically. Though impedances of extrinsic elements are small compared with those of intrinsic elements at relatively low frequencies, conventional optimizer programs assume all elements have the same accuracy and the resulting extrinsic elements fluctuate widely against their initial values.

At millimeter wave frequencies, extrinsic elements play a more important role in the overall characteristics. For example, 0.1 pF of C_{gs} and 20 pH of L_g have impedances of 1591 Ω and 0.126 Ω at 1 GHz, but 26.5 Ω and 7.56 Ω at 60 GHz. The extrinsic elements therefore heavily affect the values of the intrinsic elements determined by solving (6) to (12), at high frequencies. And the intrinsic elements can be represented as the functions of the extrinsic elements as well as frequency.

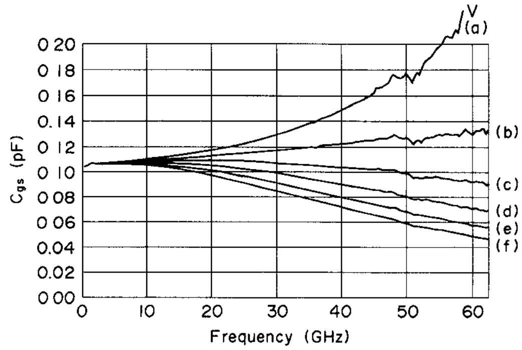

Fig. 2. Frequency characteristics of C_{gs}. (a) L_g = 0 pH, (b) L_g = 20 pH, (c) L_g = 40 pH, (d) L_g = 60 pH, (e) L_g = 80 pH, (f) L_d = 100 pH.

That is:

$$\begin{aligned} C_{gs} &= C_{gs}(\omega_i, Z_{ext}) = f_0(\omega_i, Z_{ext}) \\ R_i &= R_i(\omega_i, Z_{ext}) = f_1(\omega_i, Z_{ext}) \\ C_{gd} &= C_{gd}(\omega_i, Z_{ext}) = f_2(\omega_i, Z_{ext}) \\ g_m &= g_m(\omega_i, Z_{ext}) = f_3(\omega_i, Z_{ext}) \\ \tau &= \tau(\omega_i, Z_{ext}) = f_4(\omega_i, Z_{ext}) \\ g_{ds} &= g_{ds}(\omega_i, Z_{ext}) = f_5(\omega_i, Z_{ext}) \\ C_{ds} &= C_{ds}(\omega_i, Z_{ext}) = f_6(\omega_i, Z_{ext}). \end{aligned} \tag{13}$$

We used function names f_0 to f_6 for convenience in the following discussion.

C. Criterion of Circuit Validity

We can plot the frequency characteristics of the intrinsic elements as determined by (6) to (12) with extrinsic elements as parameters, as shown in Fig. 2 for an example. Clearly, the frequency dependence of the intrinsic elements is affected by the value of extrinsic elements. If the equivalent circuit composed of lumped elements is valid at every measurement frequency, these elements must be independent of frequency.

Conventional CAD optimizers, however, do not check circuit validity and determine extrinsic and intrinsic elements simultaneously. Extrinsic elements determined in this way often invalidate the circuit when the operating bias is changed, and some techniques have been proposed for determining extrinsic elements using additional measurements. The additional measurements are performed at DC, low frequency, and in a cold state.

Assuming that the equivalent circuit is valid for all frequency points of measurements and making use of the intrinsic elements for optimization criteria, we can determine appropriate values for extrinsic elements by iteration without complicated additional measurements.

The first candidates for criteria are the derivatives of intrinsic elements with respect to frequency, but they sometimes suffer from numerical error and measurement error. We there-

$$Z_{ext} = \begin{bmatrix} (R_g + R_s) + j\omega(L_g + L_s) & R_s + j\omega L_s \\ R_s + j\omega L_s & (R_d + R_s) + j\omega(L_d + L_s) \end{bmatrix}. \tag{2}$$

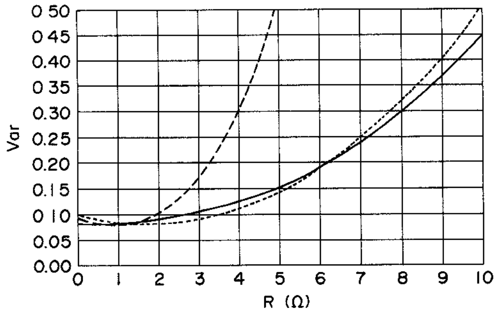

Fig. 3. Dependence of the variance on extrinsic resistances. Solid-line: R_g-variance, dashed-line: R_s-variance, dotted-line: R_d-variance.

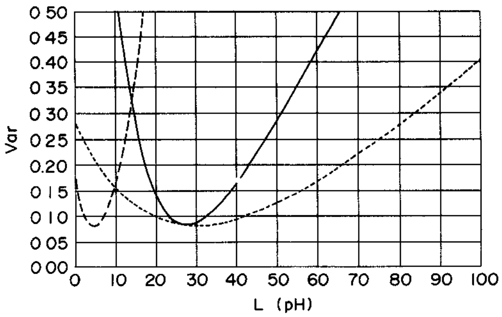

Fig. 4. Dependence of the variance on extrinsic inductances. Solid-line: L_g-variance, dashed-line: L_s-variance, dotted-line: L_d-variance.

fore chose variances as criteria. That is:

$$\varepsilon_1^k(Z_{ext}) = \frac{1}{N-1}\sum_{i=0}^{N-1} \cdot \left| f_k(\omega_i, Z_{ext}) - \overline{\sum_{i=0}^{N-1} f_k(\omega_i, Z_{ext})} \right|^2 \quad (k = 0, 1, \cdots, 6). \tag{14}$$

Fig. 3 shows the variance as a function of the extrinsic resistances, and Fig. 4 as a function of the extrinsic inductances.

Moreover, for stable calculation, the discrepancy between the measured and calculated S-parameters (15) is considered as a loose constraint. The mean values of intrinsic elements are used for calculating S-parameters.

$$\varepsilon_2(Z_{ext}) = \sum_{p=1}^{2}\sum_{q=1}^{2}\sum_{i=0}^{N-1} \cdot W_{pq}|S_{pq}^c(\omega_i, Z_{ext}) - S_{pq}^m(\omega_i)|^2. \tag{15}$$

Superscript c denotes the calculated S-parameters using (1) to (3), and m is the measured S-parameters. W_{pq} (fixed at 0.5) are the weighting factors. The extended error vector is then composed as follows.

$$\varepsilon(Z_{ext}) = \begin{pmatrix} \varepsilon_1(Z_{ext}) \\ \varepsilon_2(Z_{ext}) \end{pmatrix}. \tag{16}$$

IV. Extraction Process

A flowchart of the iterative process is shown in Fig. 5. First, the initial extrinsic resistances and inductances are subtracted from HEMT Z-parameters. The reduced Z-parameters are then converted to Y-parameters and the values of intrinsic elements

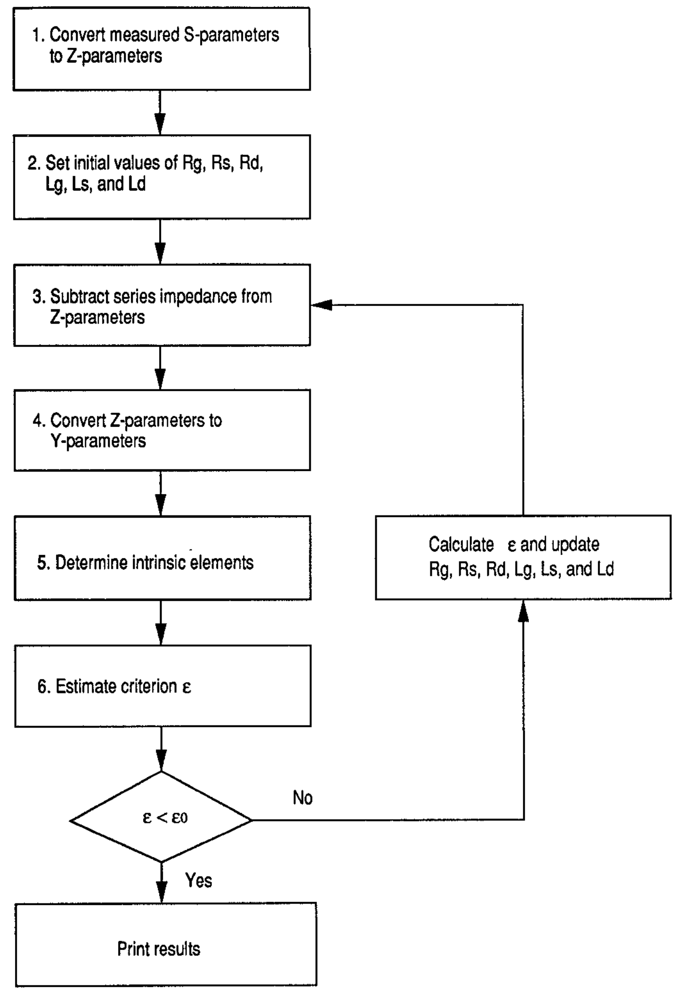

Fig. 5. Algorithm.

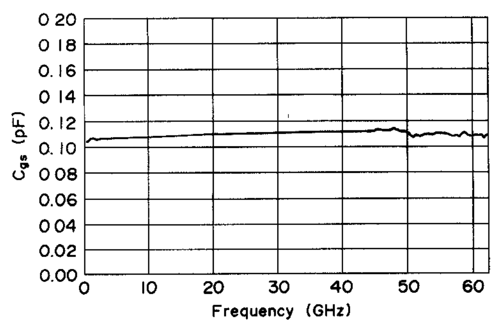

Fig. 6. Frequency characteristics of C_{gs}, $V_{gs} = 0.4$ Vp, $V_{ds} = 2$ V.

are determined using (6)–(12). Next, the extended error vector ε is estimated from (16).

The values of R_g, L_g, $\cdots$ are updated to reduce ε using the Levenberg-Marquart method. If ε is not small enough, processes three to six in Fig. 5 are repeated. The program is written in the object oriented style of $C++$, and is easy to modify for a particular equivalent circuit structure. Fig. 6 shows the obtained frequency characteristics of C_{gs} as an example.

This technique is based on iterative calculation, but eliminating additional measurements is a big advantage for example in yield estimation.

TABLE I
EXTRINSIC ELEMENTS

Elements	Initial Values	Obtained Values
Rg (Ω)	0.0	0.0157148
Lg (nH)	0.0	0 028674
Rs (Ω)	0.0	0.70738
Ls (nH)	0 0	0.00423901
Rd (Ω)	0.0	1.56885
Ld (nH)	0.0	0.0291425
Rg (Ω)	2.0	0.0161380
Lg (nH)	0.05	0.028656
Rs (Ω)	2.0	0.71358
Ls (nH)	0.05	0.00425271
Rd (Ω)	2.0	1 54451
Ld (nH)	0.05	0.0291478

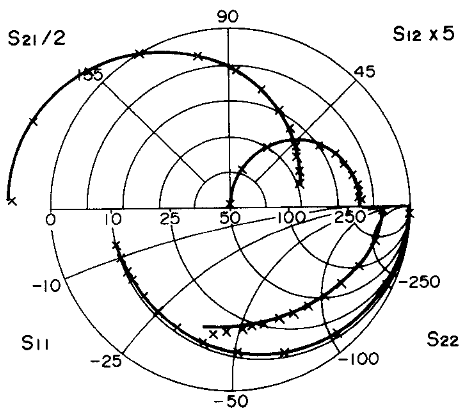

Fig. 7. HEMT S-parameters. $W_g = 100$ μm, $L_g = 0.35$ μm. Frequency: 0.5–62.5 GHz. Bias: $V_{gs} = 0.4$ V_p, $V_{ds} = 2$ V. Crosses indicate measured values and lines indicate values calculated using the equivalent circuit in Fig. 1.

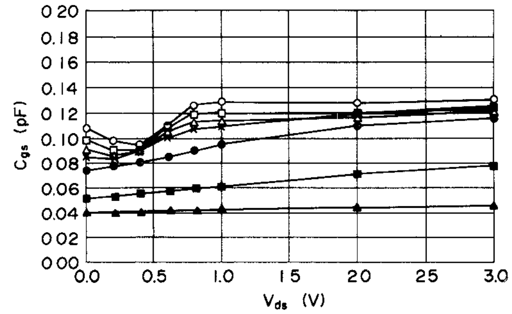

Fig. 8. Determined values of C_{gs}. —○—: $V_{gs} = 0.4$ V. —□—: $V_{gs} = 0.2$ V. —△—: $V_{gs} = 0.0$ V. —×—: $V_{gs} = 0.2$ V. —●—: $V_{gs} = 0.4$ V. —■—: $V_{gs} = 0.6$ V. —▲—: $V_{gs} = 0.8$ V.

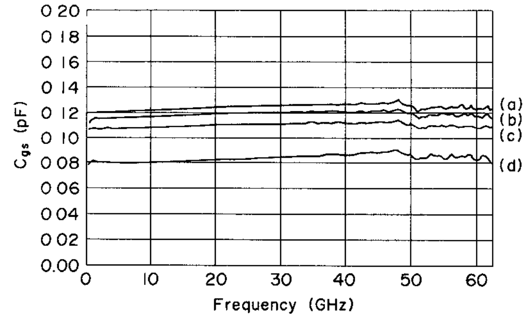

Fig. 9. Frequency characteristics of C_{gs} ($V_{gs} = -0.2$ V). (a) $V_{ds} = 3$ V, (b) $V_{ds} = 2$ V, (c) $V_{ds} = 1$ V, (d) $V_{ds} = 0$ V.

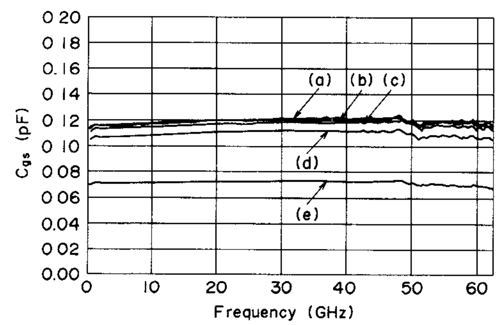

Fig. 10. Frequency characteristics of C_{gs} ($V_{ds} = 2.0$ V). (a) $V_{gs} = 0.2$ V, (b) $V_{gs} = 0.0$ V, (c) $V_{gs} = -0.2$ V, (d) $V_{gs} = -0.4$ V, (e) $V_{gs} = -0.6$ V.

V. MULTIPLE BIAS EXTRACTION

To devise a nonlinear model of HEMT's, intrinsic elements must be described as functions of bias voltages.

We therefore measured S-parameters at various bias settings, and determined extrinsic elements using the above technique on S-parameters at $V_{gs} = 0.4$ Vp, $V_{ds} = 2.0$ V. Around this bias point, the intrinsic elements of a HEMT have impedances similar to those of extrinsic elements at 60 GHz. The optimizer program then converges easily. Table I shows the extrinsic elements we obtained. Regardless of the difference of the initial values, our technique leads to a stable result. We compared values calculated from the equivalent circuit, using the extrinsic elements in Table I, with HEMT S-parameters measured up to 62.5 GHz (Fig. 7). There was good agreement between the results.

Once the extrinsic elements are known, it is easy to determine the intrinsic elements for all bias points. As an example, Fig. 8 shows the C_{gs} dependence on the gate and drain bias. We know the validity of the circuit is guaranteed by the intrinsic elements' independence of frequency. The frequency characteristics of C_{gs} (Figs. 9, 10), corresponding to Fig. 8, show that the circuit seems to be valid for all bias points.

VI. CONCLUSION

We proposed a technique to determine a HEMT equivalent circuit as the first step towards a nonlinear model. Intrinsic elements determined by a conventional analytical parameter transformation technique are described as functions of extrinsic elements, and the extrinsic elements are iteratively determined using the variance of the intrinsic elements as an optimization criterion.

We measured the S-parameters of a HEMT up to 62.5 GHz for more than 100 different bias settings, and determined the intrinsic elements at each bias point.

We are now considering a nonlinear HEMT model which we will present at a later date.

Acknowledgment

We thank the Fujitsu Compound Semiconductor Division for providing the HEMT's used in this study.

References

[1] H. A. Willing *et al.*, "A technique for predicting large-signal performance of GaAs MESFET," *IEEE Trans. Microwave Theory Tech.*, vol. 26, pp. 1017–1023, Dec. 1978.
[2] W. R. Curtice and R. L. Camisa, "Self-consistent GaAs FET models for amplifier design and device diagnostics," *IEEE Trans. Microwave Theory Tech.* vol. 32, pp. 1573–1578, Dec. 1984.
[3] Y. Takayama, "A new load-pull characterization method for microwave power transisters," in *IEEE MTT-S Dig.* 1976, pp. 218–220.
[4] R. S. Tucker and P. D. Bradley, "Computer-aided error correction of large-signal load-pull measurements," *IEEE Trans. Microwave Theory Tech.*, vol. 32, pp. 296–300, Mar. 1984.
[5] K. Nagatomo, Y. Daido, M. Shimizu, and N. Okubo, "GaAs MESFET characterization using least squares approximation by rational functions," *IEEE Trans. Microwave Theory Tech.*, vol. 41, pp. 199–205, Feb. 1993.
[6] M. Berroth and R. Bosch, "High-frequency equivalent circuit of GaAs FET's for large-signal applications," *IEEE Trans. Microwave Theory Tech.*, vol. 39, pp. 224–229, Feb. 1991.
[7] G. Dambrine, A. Cappy, F. Heliodore, and E. Playez, "A new method for determining the FET small-signal equivalent circuit," *IEEE Trans. Microwave Theory Tech.*, vol. 36, pp. 1151–1159, July 1988.
[8] H.-O. Vickes, "Determination of intrinsic FET parameters using circuit partitioning approach," *IEEE Trans. Microwave Theory Tech.*, vol. 39, pp. 363–366, Feb. 1991.
[9] R. Anholt and S. Swirhun, "Equivalent-circuit parameter extraction for cold GaAs MESFET's," *IEEE Trans. Microwave Theory Tech.*, vol. 39, pp. 1243–1247, July 1991.

Kazuo Shirakawa was born in Kyoto, Japan, in 1962. He graduated from the National Defence Academy, Yokosuka, Japan, in 1986.

In 1986, he joined Fujitsu Laboratories Ltd., Kawasaki, Japan, as an engineer in the Radio and Satellite Communication Systems Laboratory. He has been engaged in research and development of the MMIC's.

Mr. Shirakawa is a member of the Institute of Electronics, Information and Communication Engineers of Japan.

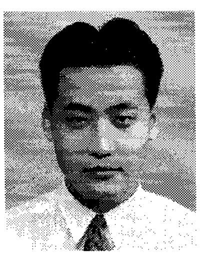

Hideyuki Oikawa was born in Miyagi, Japan, on August 28, 1972. In 1991 he graduated from Furukawa Technical High School.

In 1991 he joined Fujitsu Tohoku Digital Technology Ltd., Japan. From 1991 to 1992, he developed an oscillator in 24 GHz band. He is devoted to the development of amplifier in 60 GHz band.

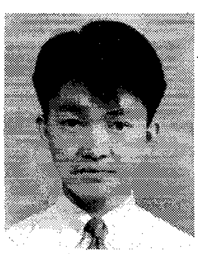

Toshihiro Shimura was born in Yamanashi, Japan, on June 26, 1967. He received the B.S. degree in physics in 1990 from Tsukuba University, Ibaraki, Japan.

He joined Fujitsu Laboratries Ltd. in April 1991 and is devoted to large-signal HEMT modeling and millimeter-wave HEMT mixer design. His current research interests include HEMT MMIC receiver design and non-linear device modeling.

Mr. Shimura is a member of the Institute of Electronics, Information and Communication Engineers of Japan.

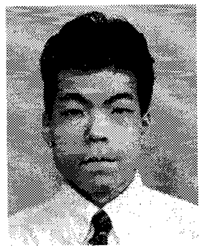

Yoshihiro Kawasaki was born in Nagasaki, Japan, on January 15, 1966. In 1986 he graduated from Sasebo Technical College and joined Fujitsu Laboratories Ltd., Japan.

He has worked on the development of waveguide circulators, waveguide to microstrip transitions, and amplifiers. He has is devoted to the development of oscillators and frequency multipliers in millimeter wave band.

Mr. Kawasaki is a member of the Institute of Electronics, Information and Communications Engineers of Japan.

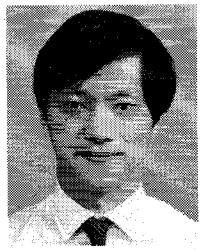

Yoji Ohashi was born in Nagoya, Japan, on January 4, 1961. He received the B.S. in physics in 1984 and M.S. in astrophysics in 1986 from Nagoya University, Nagoya, Japan.

He joined Fujitsu Laboratories Ltd. in April 1986. He has developed cryogenically cooled low-noise amplifiers for radio astronomy since 1991. He has studied noise equivalent circuits of HEMT's. His present research activities are connected with millimeter-wave HEMT monolithic integrated circuits design.

Mr Kawasaki is a member of the Institute of Electronics, Information and Communication Engineers of Japan.

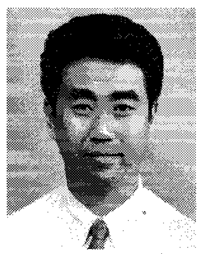

Tamio Saito (M' 92) received the B.E. in electrical and electronic systems engineering in 1982 and the M.E. in electronic engineering in 1984 from Nagaoka University of Technology, Nagaoka, Japan.

He entered Fujitsu Laboratories Ltd. in 1984, where he was engaged in microwave and millimeter-wave circuit R&D, including filters, oscillators, low-noise amplifiers and monolithic microwave integrated circuit. Since 1991, he has been working for Advanced Millimeter Wave Technologies Co. Ltd. of Yokohama, Japan, developing millimeter-wave receiver MMIC's for office communication systems.

Mr. Saito is a member of the IEEE Microwave Theory and Techniques Society and the Institute of Electronics, Information and Communication Engineers of Japan.

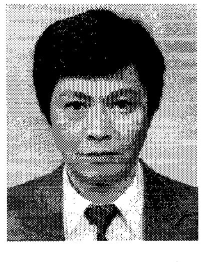

Yoshimasa Daido (M'84) received the B.S. and M.S. degrees in electrical engineering from Tokyo Institute of Technology, Tokyo, Japan, in 1968 and 1970, respectively. He received the D.E. degree from Tokyo University, Tokyo, in 1988.

He joined Fujitsu Laboratories Ltd., Kawasaki, Japan, in 1970 where he was engaged in research and development of microwave systems, optical systems, mobile communication systems and microwave amplifiers. He joined Kanazawa Institute of Technology in 1994, where he is now a professor of department of Information and Computer Engineering.

Dr. Daido is a member of the IEEE Communications Society, the IEEE Microwave Theory and Techniques Society, and the Institute of Electronics, Information and Communication Engineers of Japan.